Smad3 Signaling Promotes Fibrosis, While Preserving Cardiac and Aortic Geometry in Obese Diabetic Mice

Anna Biernacka, MD[1,*], **Michele Cavalera, PhD**[1,*], **Junhong Wang, MD**[1], **Ilaria Russo, MBiol**[1], **Arti Shinde, PhD**[1], **Ping Kong, PhD**[1], **Carlos Gonzalez-Quesada, MD**[1,2], **Vikrant Rai, MD**[1], **Marcin Dobaczewski, MD**[1,2], **Dong-Wook Lee, MD**[1], **Xiao-Fan Wang, PhD**[3], and **Nikolaos G. Frangogiannis, MD**[1,2]

[1]The Wilf Family Cardiovascular Research Institute, Department of Medicine (Cardiology), Albert Einstein College of Medicine, Bronx NY

[2]Department of Medicine, Baylor College of Medicine, Houston, TX

[3]Department of Pharmacology and Cancer Biology, Duke University School of Medicine, Durham NC

Abstract

Background—Heart failure in diabetics is associated with cardiac hypertrophy, fibrosis and diastolic dysfunction. Activation of transforming growth factor (TGF)-β/Smad3 signaling in the diabetic myocardium may mediate fibrosis and diastolic heart failure, while preserving matrix homeostasis. We hypothesized that Smad3 may play a key role in the pathogenesis of cardiovascular remodeling associated with diabetes and obesity.

Methods and Results—We generated leptin-resistant db/db Smad3 null mice (dbSKO) and db/db Smad3 +/- animals (dbShet). Smad3 haploinsufficiency did not affect metabolic function in db/db mice, but protected from myocardial diastolic dysfunction, while causing left ventricular chamber dilation. Improved cardiac compliance and chamber dilation in dbShet animals was associated with decreased cardiomyocyte hypertrophy, reduced collagen deposition and accentuated matrix metalloproteinase (MMP) activity. Attenuation of hypertrophy and fibrosis in dbShet hearts was associated with reduced myocardial oxidative and nitrosative stress. dbSKO mice had reduced weight gain and decreased adiposity associated with attenuated insulin resistance, but also exhibited high early mortality, in part due to spontaneous rupture of the ascending aorta. Ultrasound studies showed that both lean and obese Smad3 null animals had significant aortic dilation. Aortic dilation in dbSKO mice occurred despite reduced hypertension, and was associated with perturbed matrix balance in the vascular wall.

Conclusions—Smad3 mediates diabetic cardiac hypertrophy, fibrosis and diastolic dysfunction, while preserving normal cardiac geometry and maintaining the integrity of the vascular wall.

Correspondence to: Nikolaos Frangogiannis, MD, The Wilf Family Cardiovascular Research Institute, Albert Einstein College of Medicine, 1300 Morris Park Avenue Forchheimer G46B, Bronx NY 10461., Tel: 718-430-3546, Fax: 718-430-8989, nikolaos.frangogiannis@einstein.yu.edu.
*These authors contributed equally

Disclosures: None.

Keywords

obesity; diabetic cardiomyopathy; fibrosis; cardiac remodeling; TGF-β

Diabetes and obesity are associated with an increased incidence of cardiovascular disease[1,2] and are strong independent predictors of heart failure[3]. Development of heart failure in diabetics is not only due to an increased incidence of ischemic heart disease, but is also associated with a cardiomyopathy independent of coronary disease, termed diabetic cardiomyopathy. Diabetic cardiomyopathy is characterized by extensive fibrotic changes and cardiomyocyte hypertrophy leading to increased myocardial stiffness and diastolic dysfunction[4,5]. Despite its potential significance in diabetes-associated heart disease, the pathophysiologic basis of diabetic fibrosis remains poorly understood.

Extensive evidence suggests that transforming growth factor (TGF)-β is an essential fibrogenic mediator[6]; however, the relative role of TGF-β-activated pro-fibrotic pathways remains unknown. In some studies, pro-fibrotic actions of TGF-β were attributed to downstream activation of the Smad3 pathway[7,8] a key intracellular effector signal in TGF-mediated fibrosis[9]. Other investigations using models of cutaneous, pulmonary, and renal fibrosis suggested crucial fibrogenic actions of Smad-independent cascades[10,11]. In addition to its pro-fibrotic actions, TGF-β may also contribute to the development of cardiac hypertrophy, acting downstream of angiotensin II[12]. Induction and activation of TGF-β is consistently found in diabetic tissues and has been implicated in the pathogenesis of organ dysfunction; stimulation of TGF-β signaling pathways is associated with cardiac fibrosis in experimental models of type 1[13] and type 2 diabetes[14]. Accordingly, we hypothesized that activation of the Smad3 cascade in diabetic tissues, may play a critical role in the pathogenesis of hypertrophic and fibrotic remodeling in the diabetic heart.

In order to test this hypothesis, we generated obese diabetic leptin-resistant db/db mice that lack Smad3. Our findings show for the first time that Smad3 is implicated in the pathogenesis of fibrosis, cardiomyocyte hypertrophy and diastolic dysfunction in obese diabetic mice, but also exerts important homeostatic functions, preserving left ventricular and aortic geometry. Smad3 disruption resulted in chamber dilation, associated with enhanced myocardial matrix metalloproteinase (MMP) activity, suggesting that myocardial Smad3 signaling is important for preservation of the interstitial matrix and maintains chamber geometry. Moreover, complete loss of Smad3 was associated with aortic dilation and an increased incidence of spontaneous aneurysmal rupture in both lean and db/db animals suggesting an important role for Smad3 in preserving integrity of the vascular wall.

Methods

(Details are provided in the supplement)

Generation of db/db mice lacking Smad3

Animal studies were approved by the Institutional Animal Care and Use Committee at Albert Einstein College of Medicine and the Animal Protocol Review Committee at Baylor College of Medicine. Because homozygous db/db mice are sterile, we crossed heterozygous

db/+ with heterozygous Smad3 +/- (both from our own colonies on a C57BL6J background). We genotyped (using PCR) the first generation of offspring (F1) for the db and Smad3 allele and subsequently identified male and female double heterozygous mice, using them to breed the second generation of offspring (F2). For survival analysis male and female db/db mice, Smad3 -/- (Shet) mice, Smad3 -/- mice (SKO), db/db Smad3 +/- (dbShet) mice and db/db Smad3 -/- mice (dbSKO) were followed for 6 months and deaths were recorded.

Echocardiography and aortic ultrasound

WT, Shet, SKO, db/db, dbShet and dbSKO mice were imaged using a Vevo770 ultrasound system (VisualSonics, Toronto, Canada).

Assessment of body fat content

Body composition was quantitatively assessed using nuclear magnetic resonance.

Immunohistochemistry and histology

Histopathological analysis was performed using zinc formalin-fixed, paraffin-embedded hearts from 6 month-old mice.

RNA extraction and qPCR analysis

Quantitative PCR was performed using the SYBR green method on the iQ™5 Real- Time PCR Detection System. PCR primers are listed in Supplemental Table 1.

Protein extraction and western blotting

Protein was isolated from WT, db/db and dbShet hearts and Western blotting was performed.

Zymography

Matrix metalloproteinase (MMP) activity in murine WT, db/db and dbShet hearts was assessed by gelatin zymography.

Biochemical assessment of collagen content

Myocardial collagen content was measured using a hydroxyproline assay.

Assessment of plasma glucose, insulin and HOMA IR

Serum insulin levels were measured using the mouse enzyme-linked immunosorbent assay kits. Glucose levels were measured by the glucose oxidase method.

Arterial catheterization and blood pressure measurements

Invasive blood pressure measurements were performed with a Pressure:Volume analysis system.

Pressure-Volume analysis in isolated perfused hearts

Left ventricular pressure-volume analysis was performed using progressive isovolumic Langendorff retrograde perfusion of isolated murine hearts.

Assessment of oxidative stress

Myocardial reactive oxygen species (ROS) levels were measured using a fluorometric assay based on the conversion of 2′, 7′-dicholrofluorescein-diacetate (DCFDA) to the highly fluorescent DCF in the presence of ROS[15].

Statistical analysis

Data are expressed as mean ± SEM. For comparisons of two groups unpaired, 2-tailed Student's t-test using (when appropriate) Welch's correction for unequal variances was performed. The Mann-Whitney test was used for comparisons between 2 groups that did not show Gaussian distribution. For comparisons of multiple groups, 1-way ANOVA was performed followed by Tukey's multiple comparison test. The Kruskall-Wallis test, followed by Dunn's multiple comparison post-test was used when one or more groups did not show Gaussian distribution. Although adjustments for multiple comparisons in ANOVA were implemented, no additional adjustment for multiple testing was performed. Survival analysis was performed using the Kaplan-Meier method. Mortality was compared using the log rank test.

Results

1. Cardiac hypertrophy, fibrosis, and TGF-β/Smad activation in db/db hearts

db/db mice had a marked and progressive increase in left ventricular (LV) mass (Figure 1A-C) reflecting predominant hypertrophic remodeling. Female db/db mice had earlier development of cardiac hypertrophy (Supplemental Figure I). db/db hearts showed a marked increase in collagen content, a trend towards increased myocardial TGF-β1 expression and markedly higher p-Smad2 levels (Figure 1D-F).

2. Smad3 loss is associated with increased mortality in lean and in db/db mice

Follow-up to the age of 6 months showed that db/db and WT animals have comparable survival curves. Smad3 heterozygosity did not affect survival in db/db and WT animals (Figure 2A). However, both lean SKO and dbSKO animals had significantly increased mortality when compared to their corresponding Smad3+/+ littermates. Survival of dbSKO mice after 6 months of age was very rare (Figure 2B). In contrast, about 40% of SKO mice survived up to 6 months of age. Complete loss of Smad3 in db/db mice was associated with skeletal abnormalities (Supplemental Figure II).

3. Effects of Smad3 loss on weight gain, adiposity, and metabolic profile

Because Smad3 signaling is involved in adipogenesis, we examined the effects of Smad3 disruption on weight gain and adiposity in lean and in leptin-resistant, obese db/db mice. In lean mice, Smad3 loss was associated with reduced weight gain, associated with reductions in both lean and fat weight (Figure 2C-E). Percent fat was reduced only in 2 month-old Smad3 null animals, and not in 4-6 month-old mice (Figure 2F), indicating that the effects of Smad3 loss on weight gain reflected stunted growth. db/db mice had markedly increased body weight (BW) (Figure 2G). Although WT and db/db mice had comparable lean weight (Figure 2H), fat weight and percent fat were significantly higher in db/db animals (Figure

2I-J). Complete Smad3 loss in db/db mice was associated with attenuated weight gain due to significant reductions in both lean weight and fat weight (Figure 2G-I). In both lean and db/db animals, Smad3 haploinsufficiency had no effects on weight, lean weight and fat weight at 2-4 months of age. However, at 6 months, dbShet animals and Shet mice had increased adiposity. 6 month-old Shet mice had higher fat weight and fat percent content than age-matched WT mice (Figure 2E-F). Moreover, 6 month-old dbShet mice had significantly higher fat weight than corresponding db/db animals (Figure 2I). Fat percent content was comparable between db/db abd dbShet mice at all timepoints studied (Figure 2J)

Smad3 loss did not affect fasting plasma glucose, insulin levels and HOMA IR in lean animals. db/db mice exhibited hyperglycemia, hyperinsulinemia, and markedly increased HOMA IR. Complete loss of Smad3 in db/db mice was associated with significantly attenuated hyperglycemia and a trend towards reduced insulin levels and decreased HOMA IR (Figure 2K-M). In contrast, Smad3 haploinsufficiency did not affect metabolic parameters in db/db animals.

4. dbSKO mice exhibit cardiac dilation and systolic dysfunction

In lean mice, global Smad3 loss did not affect chamber dimensions and systolic function. SKO mice and WT controls had comparable LVEDD (Figure 3A, Supplemental Table 2) and LVEDV (Figure 3B); however, because of their smaller size, Smad3 null animals had a significantly higher LVEDD:BW ratio (Figure 3C). Smad3 loss in lean mice did not affect ejection fraction and LV mass (Figure 3D-E).

In db/db mice, both partial and complete Smad3 loss was associated with chamber dilation and a modest but significant reduction in ejection fraction. dbShet mice had significantly higher LVEDD and LVEDV (Figure 3F-H, Supplemental Figure III) than db/db animals. Female dbShet mice exhibited more severe chamber dilation than male animals (Supplemental Table 3). Although complete loss of Smad3 did not affect absolute chamber dimensions in db/db mice, dbSKO animals exhibited a much higher LVEDD:BW ratio (Figure 3G). Chamber dilation in dbShet and dbSKO mice was associated with mildly reduced ejection fraction (Figure 3I). Moreover, LV mass and cardiomyocyte size was significantly lower in dbSKO animals (Figure 3J-K, Supplemental Figure IV). Because dbSKO mice did not survive past the age of 6 months, comparison of ventricular dimensions and function in older animals (6-12 months of age) was limited to db/db and dbShet animals. When compared to db/db animals, dbShet had significantly increased chamber dimensions and volumes (Figure 3L-N), and exhibited a mild reduction in ejection fraction (Figure 3O), but comparable LV mass (Figure 3P). Despite reduction in ejection fraction, stroke volume and cardiac output were preserved in dbShet mice. When compared with WT animals, db/db mice had increased stroke volume and cardiac output. At 4-8 months of age, dbShet animals exhibited significantly higher cardiac output than db/db animals, likely reflecting the increased chamber dimensions (Supplemental Figure III).

5. Smad3 haploinsufficiency attenuates diastolic dysfunction in db/db mice

The effects of the db mutation on fat content, metabolic function and cardiac geometry in the absence of Smad3 are summarized in Supplemental Figure V. Because dbSKO mice

died during the first 6 months of their life, we could only study the effects of partial loss of Smad3 on diastolic function by comparing pressure:volume relations in isolated perfused db/db and dbShet hearts. At 12 months of age, db/db mice had a shift of the end-diastolic pressure:volume curve to the left and exhibited an increased chamber stiffness constant. When compared with age-matched db/db animals, dbShet mice had a shift of the end-diastolic pressure:volume curve to the right and a marked reduction in chamber stiffness constant reflecting improved ventricular compliance (Figure 4A-B).

6. dbShet mice have reduced cardiac fibrosis and enhanced MMP activity

Because Smad3 may affect cardiac geometry and function by regulating matrix metabolism, we studied the effects of Smad3 disruption on myocardial collagen deposition, MMP expression and activity. Histochemistry and a hydroxyproline assay showed that dbShet mice had markedly lower myocardial collagen content than corresponding db/db animals; however, collagen mRNA levels were not different between groups (Figure 4C-F). When compared with db/db mice, dbShet animals had increased myocardial MMP-2 and MMP-9 activity, despite exhibiting comparable MMP-2 and lower MMP-9 mRNA levels (Figure 4G-K).

7. Reduced fibrosis in dbShet hearts is associated with attenuated oxidative and nitrosative stress

When compared with WT animals, db/db mice had higher myocardial ROS levels and increased expression of 3-nitrotyrosine (Figure 5). Both partial and complete Smad3 loss attenuated myocardial oxidative stress in WT and in db/db mice (Figure 5A). Moreover, in db/db hearts, Smad3 deficiency attenuated the increase in 3-nitrotyrosine levels (Figure 5B-C).

8. Attenuated oxidative stress in dbShet myocardium is associated with reduced inflammation

When compared with db/db animals, dbShet mice had comparable myocardial Interleukin IL-1β mRNA expression, but lower levels of tumor necrosis factor-α and monocyte chemoattractant protein-1, and attenuated macrophage infiltration (Supplemental Figure VI).

9. Increased mortality in Smad3 KO is due, in part, to aortic rupture

Autopsies demonstrated that some SKO and dbSKO mice died with hemothorax, resulting from aortic rupture; aortic casts showed aneurysmal dilation (Figure 6A-C). Mortality due to aneurysmal rupture was significantly increased in dbSKO mice (44.4% of autopsied deaths) and in SKO animals (20% of deaths). Only one dbShet mouse died of aortic aneurysmal rupture. No rupture deaths were noted in Shet, db/db and WT animals.

10. Smad3 loss causes progressive aortic dilation

Aortic ultrasound showed that SKO mice had significantly increased diameter of the ascending aorta. dbSKO mice had earlier and accentuated aortic dilation. Smad3 haploinsufficiency was associated with increased aortic diameter in db/db, but not in WT animals (Figure 6D-E).

11. Aortic dilation in the absence of Smad3 is not due to increased systemic blood pressure

Because an increased hemodynamic load induces aortic dilation and increases wall tension we examined whether the aortic pathology in the absence of Smad3 is due to systemic hypertension. SKO and dbSKO mice had lower systemic blood pressure than corresponding Smad3 +/+ animals (Figure 6F-I), suggesting that aortic dilation in the absence of Smad3 is not due to hemodynamic overload.

12. SKO mice have increased SMC apoptosis and enhanced MMP expression

Because Smad3 loss may affect both matrix metabolism and SMC phenotype, we compared the morphology of the aortic matrix network and SMCs between WT and Smad3 null animals (Supplemental Figure VII). When compared with WT, Shet mice had increased aortic SMC density, while SKO mice had a trend towards increased density. Both partial and complete loss of Smad3 was associated with reduced aortic SMC size. TUNEL/α-SMA staining identified occasional apoptotic SMCs in the aortic media. Apoptotic SMCs were very rare in WT aortas; but were significantly increased in SKO and Shet animals (Supplemental Figure VII). Smad3 loss significantly increased MMP-8 and MMP-9 mRNA expression in the aorta, but did not significantly affect collagen and TIMP-1 expression levels (Supplemental Table 4).

13. dbSKO mice have attenuated aortic matrix synthesis

When compared with WT, db/db mice had comparable aortic SMC density (Supplemental Figure VIII), but exhibited significantly increased SMC size and had an increased number of apoptotic aortic SMCs. When compared with db/db, dbSKO mice had significantly reduced aortic SMC size, but comparable numbers of apoptotic SMCs. db/db mice exhibited significantly increased aortic extracellular matrix protein synthesis. When compared with db/db mice, dbShet and dbSKO had reduced collagen and tropoelastin synthesis. MMP and TIMP mRNA was also increased in db/db aortas; however the MMP-2:TIMP-1 ratio was significantly lower than in WT animals indicating predominance of matrix-preserving mediators (Supplemental Table 5).

Discussion

We demonstrate for the first time that Smad3 signaling mediates cardiac fibrosis and diastolic dysfunction in leptin-resistant diabetic mice, while preserving cardiac geometry and integrity of the vascular wall. In db/db mice, Smad3 disruption decreases fibrotic remodeling, reduces cardiac stiffness, and improves ventricular compliance; the effects of Smad3 loss are associated with decreased oxidative and nitrosative stress. Moreover, complete loss of Smad3 in both lean and obese mice is associated with aortic dilation and early death, due in part, to an increased incidence of aortic rupture.

Smad3 mediates diabetic diastolic dysfunction, while preserving chamber geometry

Cell biological investigations, animal model experiments and studies in human subjects suggest that the metabolic alterations associated with diabetes and obesity activate TGF-β/ Smad-dependent signaling. At the cellular level, high glucose potently stimulates TGF-β/

Smad3, increasing cell size and enhancing protein synthesis[16]. In experimental models of type 1 and type 2 diabetes, TGF-β/Smad3 activation is associated with tissue fibrosis. Rats with streptozotocin-induced diabetes and mice fed a high-fat diet exhibit myocardial activation of TGF-β/Smad3[17,18]. Our findings show intense myocardial activation of the TGF-β/Smad2/3 axis in obese diabetic db/db mice; increased TGF-β/Smad signaling is associated with cardiac fibrosis and development of concentric ventricular hypertrophy.

Diastolic dysfunction is the hallmark of diabetic cardiomyopathy[19,20] and may be due to cardiac hypertrophy, or to the development of interstitial fibrosis[21,22]. Our findings demonstrate that in the db/db mouse model of fibrotic diabetic cardiomyopathy, partial loss of Smad3 improves ventricular compliance (Figure 4). However, attenuated diastolic dysfunction in dbShet mice comes at a cost: Smad3 disruption increases chamber dilation (Figure 3). Whether complete absence of Smad3 further accentuates dilative remodeling is unclear. Although the LVEDD:BW ratio is markedly increased in dbSKO animals, the smaller size of mice with complete loss of Smad3 makes direct comparisons of chamber dimensions difficult to interpret. Tibial length could have provided a more appropriate method for adjustment, but was not assessed in this study. The altered geometric and functional characteristics of the ventricle are associated with reduced collagen deposition and accentuated myocardial MMP activation. Thus, in the diabetic heart, activation of Smad3 signaling promotes fibrosis, while exerting matrix-preserving actions necessary for preservation of chamber geometry. The anti-fibrotic effects of Smad3 loss may result from direct modulation of fibroblast function, or may reflect Smad-dependent actions in cardiomyocytes or vascular cells that may regulate fibroblast activation through paracrine or contact-dependent mechanisms.

The link between Smad3 and oxidative stress

Quantitative assessment of myocardial oxidative stress revealed that both partial and complete Smad3 loss markedly attenuated ROS levels and reduced 3-nitrotyrosine expression in db/db hearts (Figure 5). Oxidative stress may play an important role in the pathogenesis of the cardiomyopathy associated with diabetes and obesity acting, at least in part, through stimulation of pro-fibrotic signaling[23]. Increased ROS levels may explain some of the fibrogenic effects of Smad3 in the diabetic myocardium. The molecular links between the Smad3 cascade and the ROS system remain unknown. *In vitro* experiments have implicated Smad3 signaling in activation of oxidative stress in epithelial cells[24], hepatocytes[25] and SMCs[26] and suggested that Smad3 signaling may mediate TGF-β-induced repression of antioxidant enzymes, such as manganese superoxide dismutase (MnSOD) and catalase[24,26].

Smad3 loss results in aortic dilation and rupture

Autopsy showed that, in many cases, early death of dbSKO mice was due to spontaneous aortic rupture. Aortic ultrasound demonstrated that Smad3 loss caused significant dilation of the ascending aorta in both obese and lean animals (Figure 6). Perturbations of TGF-β signaling have been associated with aortic aneurysm formation. Overactive canonical and non-canonical TGF-β responses play a key role in aortic dilation in Marfan's syndrome[27,28]. On the other hand, disrupted TGF-β signaling has also been associated with aneurysm

formation[29,30]. Several studies have identified aortic aneurysmal disease in patients with Smad3 mutations[31]; however, whether the effects of the mutations are due to disrupted or overactive TGF-β responses remains unknown. In a Dutch family with syndromic aortic aneurysmal disease, a *SMAD3* heterozygous mutation was identified and was associated with immunohistochemical evidence of increased expression of phosphorylated Smad3[32,33]. In mice, Smad3 loss impaired aortic biomechanics and resulted in accentuated aortic inflammation and enhanced aneurysm formation upon infusion of angiotensin II[34]. Smad3 signaling may play an important role in preserving the integrity of the aortic wall by promoting matrix protein deposition and by modulating the balance between MMPs and their inhibitors[9].

What is the basis for the effects of Smad3 in the cardiovascular system?

Our findings suggest that Smad3 exerts both detrimental and protective effects on the diabetic heart and vasculature. Smad3 mediates cardiac fibrosis and diastolic dysfunction in db/db hearts, but also plays an important homeostatic role, preserving cardiac geometry and maintaining the integrity of the aortic wall. The adverse consequences of Smad3 loss in db/db mice cannot be explained by worse obesity, accentuated metabolic dysfunction or hemodynamic changes. When compared with db/db animals, dbSKO mice had significantly reduced fat content and attenuated insulin resistance. Moreover, loss of Smad3 attenuated the hypertensive response observed in db/db mice and, according to Laplace's law, would be expected to confer protection from aortic dilation and rupture by reducing wall tension. Thus, the detrimental effects of Smad3 loss on the geometry of the heart and vessels appear to involve structural perturbations of the cardiac and vascular extracellular matrix. Imbalance between matrix-preserving and matrix-degrading signals may play an important role in the pathogenesis of aortic dilation and rupture in the absence of Smad3. Moreover, effects of Smad3 disruption on vascular SMC phenotype may also be implicated (Supplemental Figures VII-VIII).

The benefits and perils of Smad3 inhibition in diabetic cardiomyopathy

Smad3 signaling is critically involved in the pathogenesis of diabetic fibrosis and diastolic dysfunction. Considering the high incidence of diastolic dysfunction in aging diabetic patients, Smad3 inhibition may be a promising therapeutic strategy to attenuate myocardial fibrosis and to protect from heart failure. However, therapeutic approaches targeting the Smad3 cascade may carry significant risks. Overzealous Smad3 inhibition may promote cardiac dilation and may accelerate aortic aneurysm formation, or cause aortic rupture in susceptible individuals.

Supplementary Material

Refer to Web version on PubMed Central for supplementary material.

Acknowledgments

References

1. Marwick TH. Diabetic heart disease. Heart. 2006; 92:296–300. [PubMed: 16159978]

2. Abel ED, Litwin SE, Sweeney G. Cardiac remodeling in obesity. Physiol Rev. 2008; 88:389–419. [PubMed: 18391168]

3. Ho JE, Lyass A, Lee DS, Vasan RS, Kannel WB, Larson MG, Levy D. Predictors of New-Onset Heart Failure: Differences in Preserved Versus Reduced Ejection Fraction. Circ Heart Fail. 2013; 6:279–286. [PubMed: 23271790]

4. Rubler S, Dlugash J, Yuceoglu YZ, Kumral T, Branwood AW, Grishman A. New type of cardiomyopathy associated with diabetic glomerulosclerosis. Am J Cardiol. 1972; 30:595–602. [PubMed: 4263660]

5. Asbun J, Villarreal FJ. The pathogenesis of myocardial fibrosis in the setting of diabetic cardiomyopathy. J Am Coll Cardiol. 2006; 47:693–700. [PubMed: 16487830]

6. Biernacka A, Dobaczewski M, Frangogiannis NG. TGF-beta signaling in fibrosis. Growth Factors. 2011; 29:196–202. [PubMed: 21740331]

7. Bujak M, Ren G, Kweon HJ, Dobaczewski M, Reddy A, Taffet G, Wang XF, Frangogiannis NG. Essential Role of Smad3 in Infarct Healing and in the Pathogenesis of Cardiac Remodeling. Circulation. 2007; 116:2127–38. [PubMed: 17967775]

8. Flanders KC. Smad3 as a mediator of the fibrotic response. Int J Exp Pathol. 2004; 85:47–64. [PubMed: 15154911]

9. Dobaczewski M, Bujak M, Li N, Gonzalez-Quesada C, Mendoza LH, Wang XF, Frangogiannis NG. Smad3 signaling critically regulates fibroblast phenotype and function in healing myocardial infarction. Circ Res. 2010; 107:418–28. [PubMed: 20522804]

10. Bhattacharyya S, Chen SJ, Wu M, Warner-Blankenship M, Ning H, Lakos G, Mori Y, Chang E, Nihijima C, Takehara K, Feghali-Bostwick C, Varga J. Smad-independent transforming growth factor-beta regulation of early growth response-1 and sustained expression in fibrosis: implications for scleroderma. Am J Pathol. 2008; 173:1085–99. [PubMed: 18772333]

11. Wang S, Wilkes MC, Leof EB, Hirschberg R. Imatinib mesylate blocks a non-Smad TGF-beta pathway and reduces renal fibrogenesis in vivo. Faseb J. 2005; 19:1–11. [PubMed: 15629889]

12. Huntgeburth M, Tiemann K, Shahverdyan R, Schluter KD, Schreckenberg R, Gross ML, Modersheim S, Caglayan E, Muller-Ehmsen J, Ghanem A, Vantler M, Zimmermann WH, Bohm M, Rosenkranz S. Transforming growth factor beta(1) oppositely regulates the hypertrophic and contractile response to beta-adrenergic stimulation in the heart. PLoS One. 2011; 6:e26628. [PubMed: 22125598]

13. Westermann D, Rutschow S, Jager S, Linderer A, Anker S, Riad A, Unger T, Schultheiss HP, Pauschinger M, Tschope C. Contributions of inflammation and cardiac matrix metalloproteinase activity to cardiac failure in diabetic cardiomyopathy: the role of angiotensin type 1 receptor antagonism. Diabetes. 2007; 56:641–6. [PubMed: 17327431]

14. Lenski M, Kazakov A, Marx N, Bohm M, Laufs U. Effects of DPP-4 inhibition on cardiac metabolism and function in mice. J Mol Cell Cardiol. 2011; 51:906–18. [PubMed: 21871459]

15. Riehle C, Wende AR, Zaha VG, Pires KM, Wayment B, Olsen C, Bugger H, Buchanan J, Wang X, Moreira AB, Doenst T, Medina-Gomez G, Litwin SE, Lelliott CJ, Vidal-Puig A, Abel ED. PGC-1beta deficiency accelerates the transition to heart failure in pressure overload hypertrophy. Circ Res. 2011; 109:783–93. [PubMed: 21799152]

16. Wu L, Derynck R. Essential role of TGF-beta signaling in glucose-induced cell hypertrophy. Dev Cell. 2009; 17:35–48. [PubMed: 19619490]

17. Talior-Volodarsky I, Connelly KA, Arora PD, Gullberg D, McCulloch CA. alpha11 integrin stimulates myofibroblast differentiation in diabetic cardiomyopathy. Cardiovasc Res. 2012; 96:265–75. [PubMed: 22869616]

18. Wang HT, Liu CF, Tsai TH, Chen YL, Chang HW, Tsai CY, Leu S, Zhen YY, Chai HT, Chung SY, Chua S, Yen CH, Yip HK. Effect of obesity reduction on preservation of heart function and attenuation of left ventricular remodeling, oxidative stress and inflammation in obese mice. J Transl Med. 2012; 10:145. [PubMed: 22784636]

19. Uusitupa MI, Mustonen JN, Airaksinen KE. Diabetic heart muscle disease. Ann Med. 1990; 22:377–86. [PubMed: 2076269]

20. Mandavia CH, Aroor AR, Demarco VG, Sowers JR. Molecular and metabolic mechanisms of cardiac dysfunction in diabetes. Life Sci. 2013; 92:601–8. [PubMed: 23147391]

21. Koitabashi N, Danner T, Zaiman AL, Pinto YM, Rowell J, Mankowski J, Zhang D, Nakamura T, Takimoto E, Kass DA. Pivotal role of cardiomyocyte TGF-beta signaling in the murine pathological response to sustained pressure overload. J Clin Invest. 2011; 121:2301–12. [PubMed: 21537080]

22. Cavalera M, Wang J, Frangogiannis NG. Obesity, metabolic dysfunction, and cardiac fibrosis: pathophysiological pathways, molecular mechanisms, and therapeutic opportunities. Transl Res. 2014; S1931-5244(14):00164–9.

23. Ilkun O, Boudina S. Cardiac dysfunction and oxidative stress in the metabolic syndrome: an update on antioxidant therapies. Curr Pharm Des. 2013; 19:4806–17. [PubMed: 23323621]

24. Bakin AV, Stourman NV, Sekhar KR, Rinehart C, Yan X, Meredith MJ, Arteaga CL, Freeman ML. Smad3-ATF3 signaling mediates TGF-beta suppression of genes encoding Phase II detoxifying proteins. Free Radic Biol Med. 2005; 38:375–87. [PubMed: 15629866]

25. Black D, Lyman S, Qian T, Lemasters JJ, Rippe RA, Nitta T, Kim JS, Behrns KE. Transforming growth factor beta mediates hepatocyte apoptosis through Smad3 generation of reactive oxygen species. Biochimie. 2007; 89:1464–73. [PubMed: 17936489]

26. Michaeloudes C, Sukkar MB, Khorasani NM, Bhavsar PK, Chung KF. TGF-beta regulates Nox4, MnSOD and catalase expression, and IL-6 release in airway smooth muscle cells. Am J Physiol Lung Cell Mol Physiol. 2010; 300:L295–304. [PubMed: 21131394]

27. Neptune ER, Frischmeyer PA, Arking DE, Myers L, Bunton TE, Gayraud B, Ramirez F, Sakai LY, Dietz HC. Dysregulation of TGF-beta activation contributes to pathogenesis in Marfan syndrome. Nat Genet. 2003; 33:407–11. [PubMed: 12598898]

28. Gillis E, Van Laer L, Loeys BL. Genetics of Thoracic Aortic Aneurysm: At the Crossroad of Transforming Growth Factor-beta Signaling and Vascular Smooth Muscle Cell Contractility. Circ Res. 2013; 113:327–40. [PubMed: 23868829]

29. Wang Y, Ait-Oufella H, Herbin O, Bonnin P, Ramkhelawon B, Taleb S, Huang J, Offenstadt G, Combadiere C, Renia L, Johnson JL, Tharaux PL, Tedgui A, Mallat Z. TGF-beta activity protects against inflammatory aortic aneurysm progression and complications in angiotensin II-infused mice. J Clin Invest. 2010; 120:422–32. [PubMed: 20101093]

30. Lindsay ME, Schepers D, Bolar NA, Doyle JJ, Gallo E, Fert-Bober J, Kempers MJ, Fishman EK, Chen Y, Myers L, Bjeda D, Oswald G, Elias AF, Levy HP, Anderlid BM, Yang MH, Bongers EM, Timmermans J, Braverman AC, Canham N, Mortier GR, Brunner HG, Byers PH, Van Eyk J, Van Laer L, Dietz HC, Loeys BL. Loss-of-function mutations in TGFB2 cause a syndromic presentation of thoracic aortic aneurysm. Nat Genet. 2012; 44:922–7. [PubMed: 22772368]

31. Regalado ES, Guo DC, Villamizar C, Avidan N, Gilchrist D, McGillivray B, Clarke L, Bernier F, Santos-Cortez RL, Leal SM, Bertoli-Avella AM, Shendure J, Rieder MJ, Nickerson DA, Milewicz DM. Exome sequencing identifies SMAD3 mutations as a cause of familial thoracic aortic aneurysm and dissection with intracranial and other arterial aneurysms. Circ Res. 2011; 109:680–6. [PubMed: 21778426]

32. van de Laar IM, Oldenburg RA, Pals G, Roos-Hesselink JW, de Graaf BM, Verhagen JM, Hoedemaekers YM, Willemsen R, Severijnen LA, Venselaar H, Vriend G, Pattynama PM, Collee M, Majoor-Krakauer D, Poldermans D, Frohn-Mulder IM, Micha D, Timmermans J, Hilhorst-Hofstee Y, Bierma-Zeinstra SM, Willems PJ, Kros JM, Oei EH, Oostra BA, Wessels MW, Bertoli-Avella AM. Mutations in SMAD3 cause a syndromic form of aortic aneurysms and dissections with early-onset osteoarthritis. Nat Genet. 2011; 43:121–6. [PubMed: 21217753]

33. van der Linde D, van de Laar IM, Bertoli-Avella AM, Oldenburg RA, Bekkers JA, Mattace-Raso FU, van den Meiracker AH, Moelker A, van Kooten F, Frohn-Mulder IM, Timmermans J, Moltzer E, Cobben JM, van Laer L, Loeys B, De Backer J, Coucke PJ, De Paepe A, Hilhorst-Hofstee Y, Wessels MW, Roos-Hesselink JW. Aggressive cardiovascular phenotype of aneurysms-osteoarthritis syndrome caused by pathogenic SMAD3 variants. J Am Coll Cardiol. 2012; 60:397–403. [PubMed: 22633655]

34. Tan CK, Tan EH, Luo B, Huang CL, Loo JS, Choong C, Tan NS. SMAD3 deficiency promotes inflammatory aortic aneurysms in angiotensin II-infused mice via activation of iNOS. J Am Heart Assoc. 2013; 2:e000269. [PubMed: 23782924]

Clinical Perspective

Heart failure with preserved ejection fraction is a major cause of morbidity and mortality in patients with diabetes and obesity. Although cardiac fibrosis is prominent in diabetics and has been implicated in the pathogenesis of diastolic dysfunction, the molecular signals involved in fibrotic remodeling of the diabetic myocardium remain unknown. The Transforming Growth Factor (TGF)-β/Smad pathway is activated in diabetic tissues and may be involved in fibrosis. Our study demonstrates for the first time an important role for Smad3 signaling in diabetes-associated cardiac fibrosis and diastolic dysfunction. Genetic disruption of Smad3 improves ventricular compliance, reducing cardiomyocyte hypertrophy and decreasing fibrosis in obese diabetic mice. These effects are associated with increased myocardial activation of matrix metalloproteinases and with attenuated cardiac oxidative stress. Although Smad3 mediates fibrosis and increases myocardial stiffness in diabetic animals, it is also important in preservation of cardiac and aortic geometry. Smad3 loss in diabetic mice is associated with modest, non-progressive ventricular dilation, and with aortic aneurysm formation, despite a reduction in systemic blood pressure. Thus, a word of caution should be raised regarding the potential use of Smad3 inhibition to protect diabetics from cardiac fibrosis and diastolic heart failure. Overzealous Smad3 blockade may have catastrophic effects in vulnerable individuals, causing progressive aortic dilation and rupture.
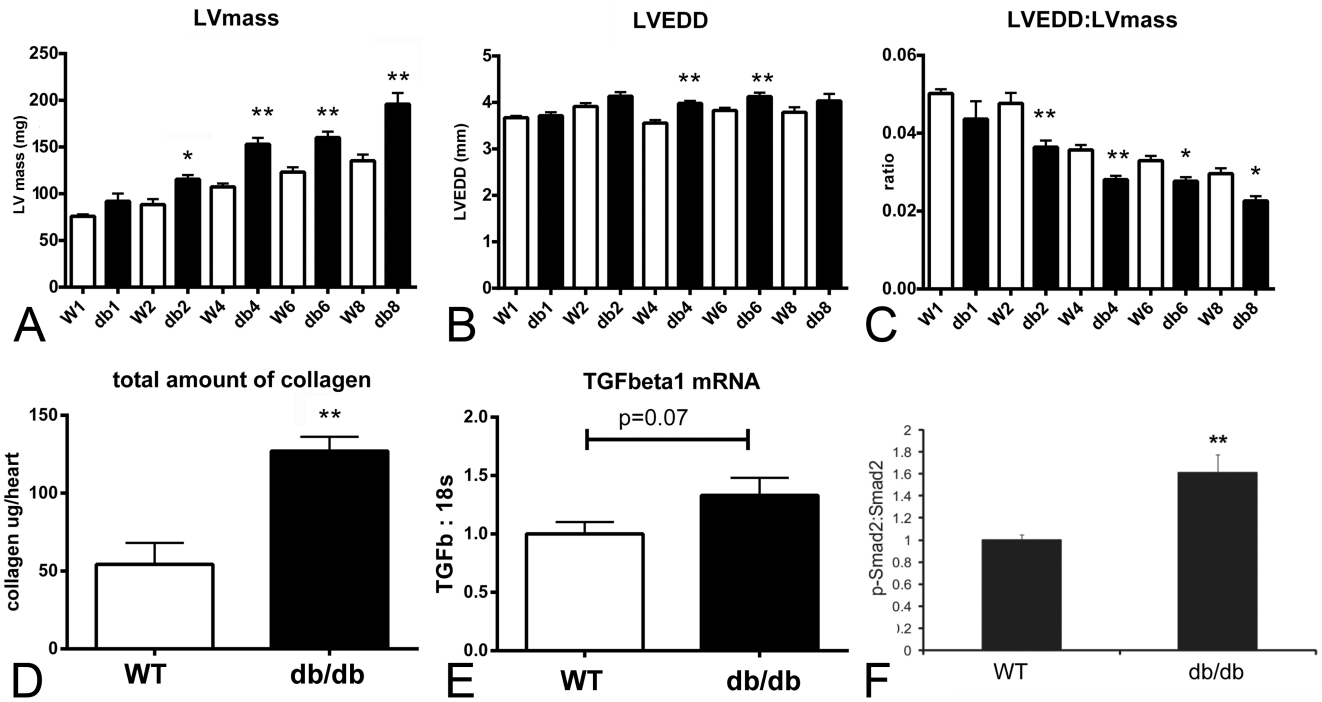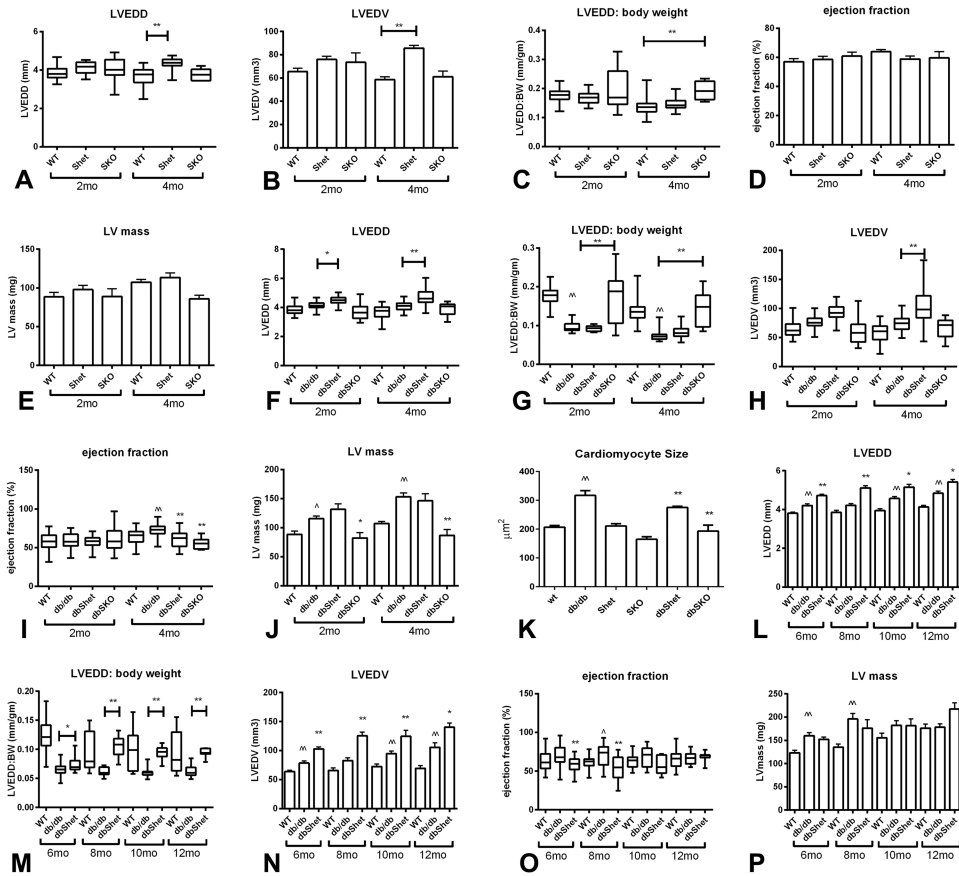
Figure 1.
db/db mice exhibit cardiac hypertrophy and fibrosis associated with activation of TGF-β/Smad. **A**. db/db mice had significantly higher LV mass than corresponding lean WT animals. **B**. db/db and WT animals had comparable LVEDD between 1-2 months of age and exhibited only subtle increases in chamber dimensions at 4-6 months. **C**. LVEDD:LVmass ratio was markedly lower in db/db animals reflecting predominant hypertrophic remodeling. **D**. 6 month-old db/db hearts were fibrotic showing a marked increase in collagen content (measured with a hydroxyproline assay). **E.** There was a trend towards increased TGF-β1 mRNA expression in db/db hearts. **F**. Expression of p-Smad2 was increased in db/db myocardium (*p<0.05, **p<0.01 vs. WT). (echocardiography WT n=25-73/group, db/db n=14-44/group; collagen n=8/group; mRNA n=15/group; western blotting n=8/group).
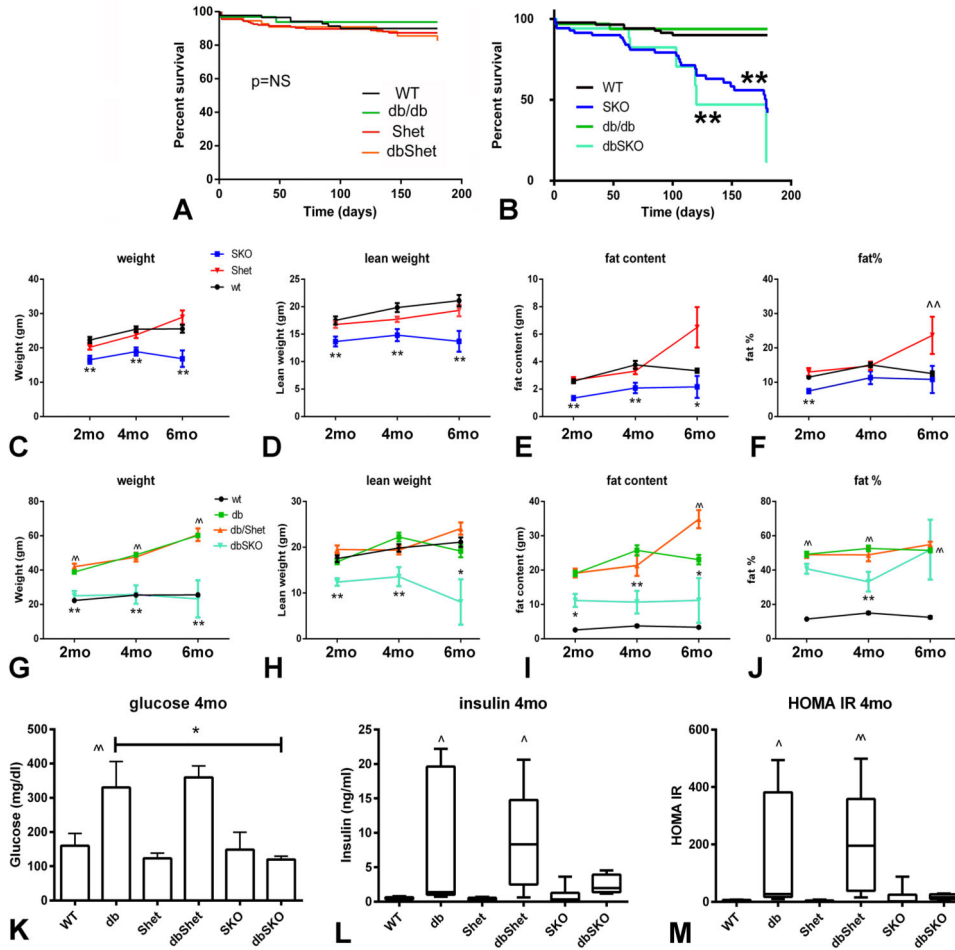
Figure 2.

Smad3 loss increases mortality in both lean and db/db mice and is associated with attenuated weight gain and reduced adiposity. **A**. WT mice, db/db mice, Shet and dbShet mice had comparable survival curves. **B**. When compared with WT animals, Smad3 knockout mice (SKO) had higher mortality (**p<0.01). In comparison to db/db, db/db Smad3 -/- (dbSKO) animals had higher mortality (**p<0.01). All dbSKO mice died before 6 months of age. **C**. SKO mice had significantly lower body weight than corresponding lean WT animals (**p<0.01). **D-E**: Reduced weight in SKO mice was due to reductions in both lean weight **(D)** and fat content **(E)**. **F.** 2 month-old SKO mice had lower fat % content than WT animals (**p<0.01); however at 4 and 6 months, fat % was not significantly different between WT and SKO. Shet animals had increased fat % content at 6 months of age (^^p<0.01 vs. WT). **G.** db/db mice had a marked increase in body weight at 2-6 months of age (^^p<0.01 vs. age-matched WT mice). In comparison to db/db, dbSKO mice had markedly lower body weight (**p<0.01). **H-I.** Reduced weight gain in dbSKO mice was due to reductions in both lean weight and fat content (*p<0.05, **p<0.01 vs. db/db). At 6 months of age, dbShet mice had a statistically significant increase in fat content when compared with db/db animals (^^p<0.01 vs. db/db). **J.** Percent fat content was markedly increased in db/db animals (^^p<0.01 vs. corresponding WT). However, Smad3 loss in dbSKO animals was associated

with reduced percent fat content only at 4 months of age, suggesting that lower body weight in the absence of Smad3 was predominantly related to stunted growth. **K**. db/db and dbShet mice had significantly increased plasma glucose levels when compared with WT animals (^^p<0.01 vs. WT); dbSKO mice had attenuated hyperglycemia. **L**. Insulin levels were also markedly increased in db/db and dbShet animals (^p<0.05 vs. WT); however dbSKO mice had comparable insulin levels with lean WT controls. **M.** HOMA-IR was also significantly higher in db/db and in dbShet mice when compared with corresponding WT controls (^p<0.05, ^^p<0.01 vs. WT); in contrast, in dbSKO mice, HOMA IR was comparable with WT animals suggesting attenuated insulin resistance. Survival: WT n=86, Shet n=175, SKO n=70, db/db n=32, dbShet n=55, dbSKO n=17; weight and adiposity: WT n=14, db/db n=16, dbShet n=25, dbSKO n=19 (2mo) n=9 (4mo), Shet n=16, SKO n=19 (2mo) n=17 (4mo); metabolic analysis: n=6.

Figure 3.

Smad3 heterozygosity in db/db mice is associated with increased chamber dilation and a modest reduction in ejection fraction. Systolic function, dilative and hypertrophic remodeling were compared between lean WT mice and corresponding Shet and SKO animals (**A-E**), and between db/db, dbShet and dbSKO mice (**F-J**) using echocardiography. Panels K-O show comparison of echocardiographic endpoints between WT, db and dbShet animals at 6 and 12 months of age (at these timepoints comparison with SKO and dbSKO mice is not possible due to their early mortality) **A-E**: Shet and SKO mice had modest chamber dilation with preserved systolic function. **A**: At 4 months of age, Shet mice had higher LVEDD than WT animals (**p<0.01). **B**: LVEDV was significantly higher in Shet animals at 4 months of age. **C**: When adjusted to body weight, SKO animals also exhibited an increase in LVEDD:BW ratio. **D**. Ejection fraction was comparable between groups at 2 and 4 months of age. **E**: No statistically significant differences in LV mass were noted. **F**: dbShet mice had a significantly higher LVEDD than db/db animals. **G**: dbSKO mice had significantly increased LVEDD:body weight ratio. **H**. LVEDV was significantly higher in dbShet mice at 4 months of age. **I**. When compared with age-matched WT animals, db/db mice had increased ejection fraction (^^p<0.01 vs WT). When compared with db/db animals, dbShet mice and dbSKO animals had a modest, but significant reduction in ejection fraction (**p<0.01 vs db/db). **J-K**: db/db mice had increased LV mass and higher cardiomyocyte size than age-matched lean controls (^p<0.05, ^^p<0.01 vs. WT). dbSKO mice had attenuated LV hypertrophy, suggested by reduced LV mass (J) and decreased

cardiomyocyte size (K) (*p<0.05, **p<0.01 vs. db/db). **L-N**: At 6-12 months of age, dbShet mice had persistent chamber dilation (*p<0.05, **p<0.01 vs. age-matched db/db) without significant progression of dilative remodeling **O**. Ejection fraction was significantly lower in dbShet mice at 6 and 8 months of age (**p<0.01 vs. db/db); however progressive systolic dysfunction was not observed. **P**: In comparison to WT animals, db/db mice had significantly higher LV mass at 6-8 months of age (^^p<0.01 vs. WT). dbShet mice and db/db mice had comparable LV mass at 6 and 12 months of age (2 mo of age: WT n=14, Shet=26, SKO n=10, db/db n=16, dbShet n=15, dbSKO n=19; 4mo of age: WT n=45, Shet n=27, SKO n=6, db/db n=42, dbShet n=16, dbSKO n=10, Shet n=16) (^p<0.05, ^^p<0.01 vs. age-matched WT)..
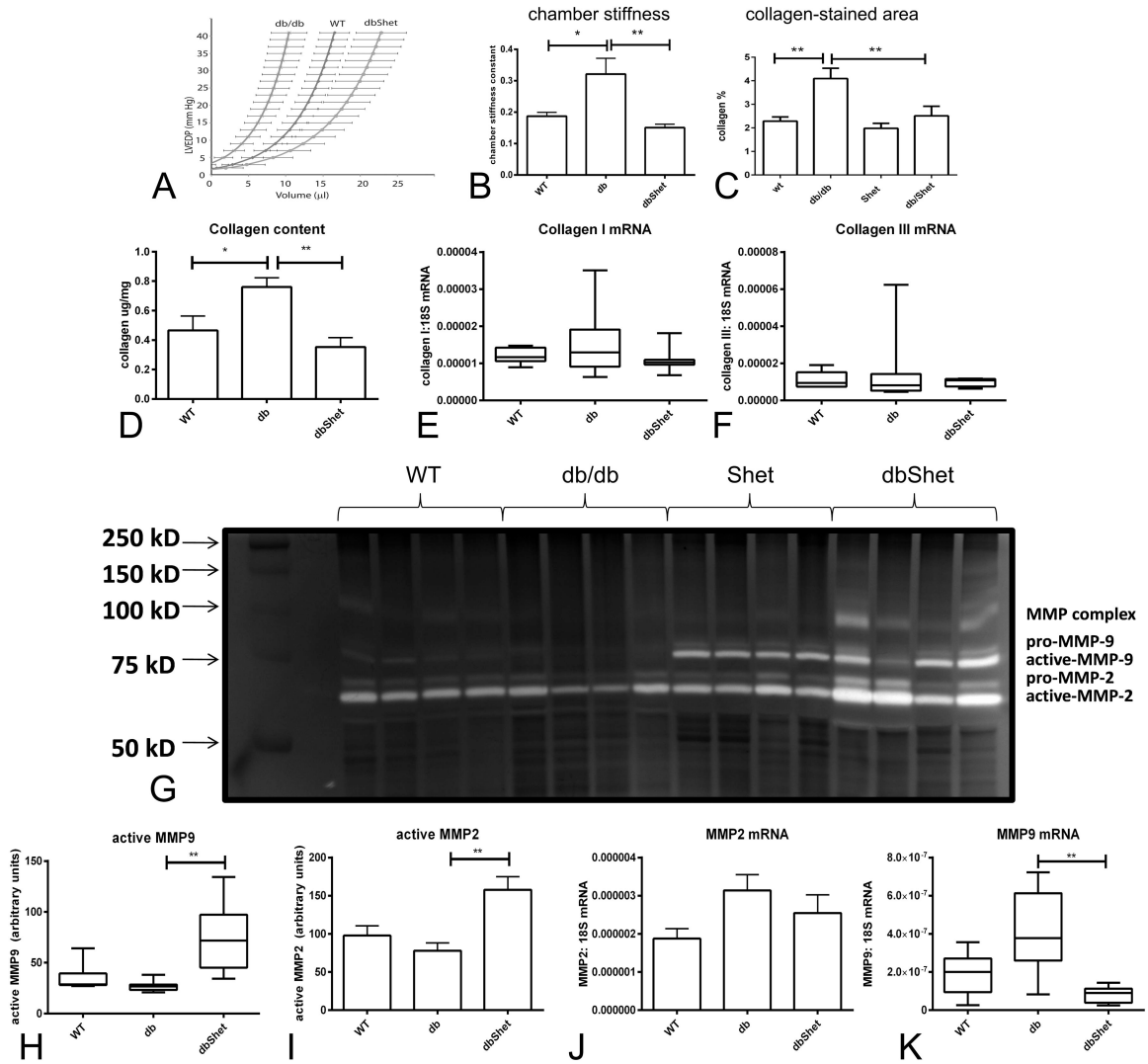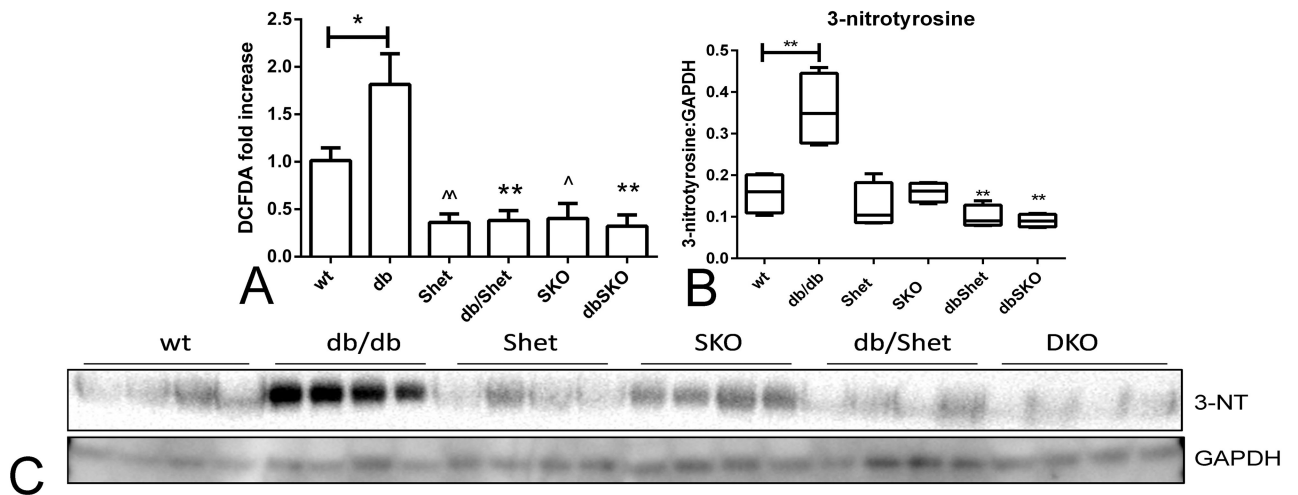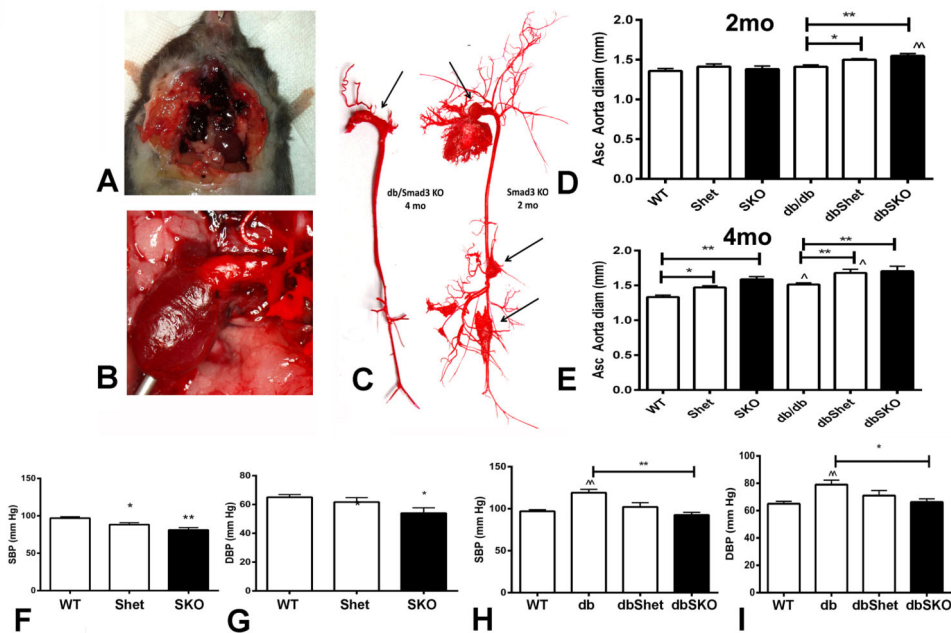
Figure 4.

dbShet mice exhibit attenuated diastolic dysfunction associated with reduced matrix deposition and increased MMP activity. **A**. Pressure:volume relations in 12 month-old animals demonstrated that db/db mice exhibit a shift of the curve to the left and that dbShet hearts had improved compliance. **B**. Left ventricular chamber stiffness constant was increased in db/db mice. Partial loss of Smad3 reduced the chamber stiffness constant in db/db animals (*p<0.05, **p<0.01). **C-D**. Improved diastolic function in dbShet hearts was associated with reduced collagen content, assessed through Sirius red staining (**C**) and through a hydroxyproline assay (**D**). **E-F**. Reduced collagen in dbShet hearts was not due to differences in collagen transcription. **G-I**. dbShet animals had increased myocardial MMP9 (**H**) and MMP2 (**I**) activity, assessed with zymography (**G**). Accentuated MMP activity in dbShet hearts was not due to increased MMP2 (**J**) or MMP9 (**K**) transcription.

Figure 5.
A. Smad3 loss attenuates oxidative and nitrosative stress in WT and db/db hearts. DCFDA assay showed that db/db hearts had increased ROS levels when compared with age-matched WT hearts (*p<0.05 vs WT). Partial or complete loss of Smad3 markedly reduced myocardial ROS levels in WT and in db/db animals (^p<0.05, ^^p<0.01 vs. WT; **p<0.01 vs. db/db, n=6/group). **B-C**. 3-nitrotyrosine expression was markedly increased in db/db hearts (**p<0.01 vs WT). Smad3 loss in db/db mice resulted in attenuated 3-nitrotyrosine expression (**p<0.01 vs. db/db).

Figure 6.
SKO and dbSKO mice had aortic dilation and a high incidence of spontaneous rupture. **A**. Hemothorax in a 2 month-old SKO mouse that died spontaneously. **B**. Dilated ascending aorta in a dbSKO animal. **C**. Casts of the aorta show dilation and aneurysm formation (arrows) in a 4 month-old dbSKO and a 2 month-old SKO mouse. **D**. Ultrasound showed that at 2 months of age, the ascending aorta was significantly dilated in dbShet and in dbSKO mice (*p<0.05, **p<0.01 vs. db/db). **E**. At 4 months of age, lean Shet and SKO mice had increased aortic diameter (*p<0.05, **p<0.01 vs. WT). dbShet and dbSKO exhibited increased aortic dimensions in comparison to db/db animals (**p<0.01 vs. db/db). (WT n=10, Shet n=11, SKO n=16; db/db n=14, dbShet n=13, dbSKO n=9). **F-I.** Aortic dilation in SKO and dbSKO mice was not due to increased systemic blood pressure. When compared with 4-month old WT animals, age-matched Shet and SKO mice had lower systolic **(F)** and diastolic **(G)** blood pressure (*p<0.05, **p<0.01 vs. WT). 4 month-old db/db mice had higher systolic **(H)** and diastolic **(I)** blood pressure than lean WT animals (^^p<0.01 vs. WT). Smad3 loss in db/db mice protected from increase in systemic blood pressure **(H, I)** (**p<0.01). (WT n=8, db/db n=6; dbShet, dbSKO, SKO, Shet n=5).